

Extraordinary Electrical Conductance of Non-conducting Polymers Under Vibrational Strong Coupling

*Sunil Kumar^{1#}, Subha Biswas^{1#}, Umar Rashid¹, Kavya S. Mony¹, Robrecht M. A. Vergauwe²,
Veerabhadrarao Kaliginedi^{1*}, Anoop Thomas^{1*}*

¹Inorganic and Physical Chemistry, Indian Institute of Science; Bengaluru, India

²Nanoscience Center and Department of Chemistry, University of Jyväskylä; Jyväskylä, Finland.

*Correspondence to: vkaliginedi@iisc.ac.in; athomas@iisc.ac.in

[#]These authors contributed equally

Abstract:

Achieving vibrational mode selectivity to control molecular properties is a challenging task that has become greatly facilitated by vibrational strong coupling. Here we show that strongly coupling the vibrational transitions of polystyrene (PS) and poly (benzyl-methacrylate) (PBMA) to the vacuum electromagnetic field of the cavity enhances the electrical conductance by several orders of magnitude. Remarkably, the extraordinary enhancement of electrical conductance in PS is mode-selective to the vibrational strong coupling (VSC) of the aromatic ring out-of-plane bending transitions corresponding to B_2 symmetry. The delocalized hybrid light-matter states formed under VSC could promote extended vibronic coherence, enhancing the electrical conductance. These experiments are done without any light excitation, demonstrating the role of electromagnetic vacuum fluctuations in controlling the long-range quantum coherent transport in molecular materials.

Main Text:

A fascinating aspect of quantum electrodynamics is that the radiation field can interact with matter through its electromagnetic vacuum fluctuations.¹ Although it is difficult to probe these fluctuations by direct measurements,² spontaneous emission, often thought of as an intrinsic matter property, arises fundamentally from the interaction of the matter with this ubiquitous field. The density and the availability of radiation modes are modified significantly by confining the field, for instance, using a Fabry-Perot cavity.¹ Unlike in free space, the molecules inside the cavity may interact collectively with the allowed cavity modes and falls under a weak or strong light-matter coupling regime.³ Under strong coupling, electromagnetic vacuum fluctuations can interact with the molecular electronic/vibrational absorption transition dipole by exchanging virtual photons at a rate faster than other dissipations to form hybrid light-matter states known as

polaritonic states (P+ and P-). The latter are separated by the vacuum Rabi splitting energy ($\hbar\Omega_R$), as schematically shown in Fig. 1A, with vibrational strong coupling as the example. Remarkably, the coherent polaritonic states formed under the electronic strong coupling (ESC) or VSC can introduce modifications to the matter properties,⁴⁻⁶ chemical reactivity landscapes,^{7,8} intermolecular interactions,⁹⁻¹¹ and magnetic properties,^{12,13} of molecules and materials.

Experiments have shown that the electrical conductivity and energy transport of organic molecules can be enhanced by hybridizing their electronic transitions under the electronic strong coupling regime.¹⁴⁻²⁰ However, the role of vibrational strong coupling in organic electronics is unexplored, although vibronic coherence,^{21,22} and vibrational mode selective excitation²³⁻²⁶ are known to modify electrical transport in molecular systems. In typical molecules, the disorder can limit the extent of vibronic coherence.²⁷ Moreover, vibrational mode selective excitation often demands cryogenic temperatures to obtain the transient enhancement in conductance.²³ Coherent collective coupling of molecules with a cavity mode can be achieved at room temperature through VSC without the necessity of light excitation; therefore, VSC should provide a stationary alternative to the transient mode selective vibrational excitation. To check this hypothesis, we designed experiments to study electrical conductance through PS and PBMA under VSC. The choice of PS as the active material is based on the following considerations: (i) the presence of pendant ring interactions,²⁸ and (ii) the presence of aromatic ring vibrational transitions that facilitates the vibronic coupling.²⁹ PBMA also satisfies similar criteria. Remarkably, we observe that the VSC of the aromatic ring out-of-plane bending vibrational modes of PS and PBMA induces extraordinary enhancement in electrical conductance by ~6 orders of magnitude compared to uncoupled (non-cavity) polymers.

Vibrational strong coupling of PS is achieved by placing the PS layer between two flat Au mirrors. Typically, it is done by spin coating a homogenous solution of PS in toluene onto the bottom Au mirror (10 nm thick) supported on an intrinsic Si wafer and subsequent closing of the cavity by sputtering another Au mirror (10 nm thick) on top. The cavity path length (thickness of the PS) is varied across samples to obtain the desired on- and off-resonance condition between cavity modes and PS vibrational transitions. We did the XPS depth profile analysis of a series of on- and off-resonance cavities of different PS thicknesses to confirm that the sputtering of the top mirror does not induce any diffusion of Au atoms into the PS (Fig S2). X-ray reflectivity studies reported a similar observation in the literature.³⁰ Additional complementary experiments³⁰ by transfer printing

Au film instead of sputtering yield the same results as described further down. The non-cavity PS refers to a reference PS film spin-coated on the bottom Au (Fig.S5). Spin coating of the concentrated PS solution can sometimes create pathlength inhomogeneity in the sample; typically, the central region is homogenous, and the sides have low finesse modes due to thickness heterogeneity (Fig.S6). The spectral and electrical data presented here correspond to the measurements done in the homogeneous region of the cavity. Refer to Supplementary Materials for sample preparation and characterization details.

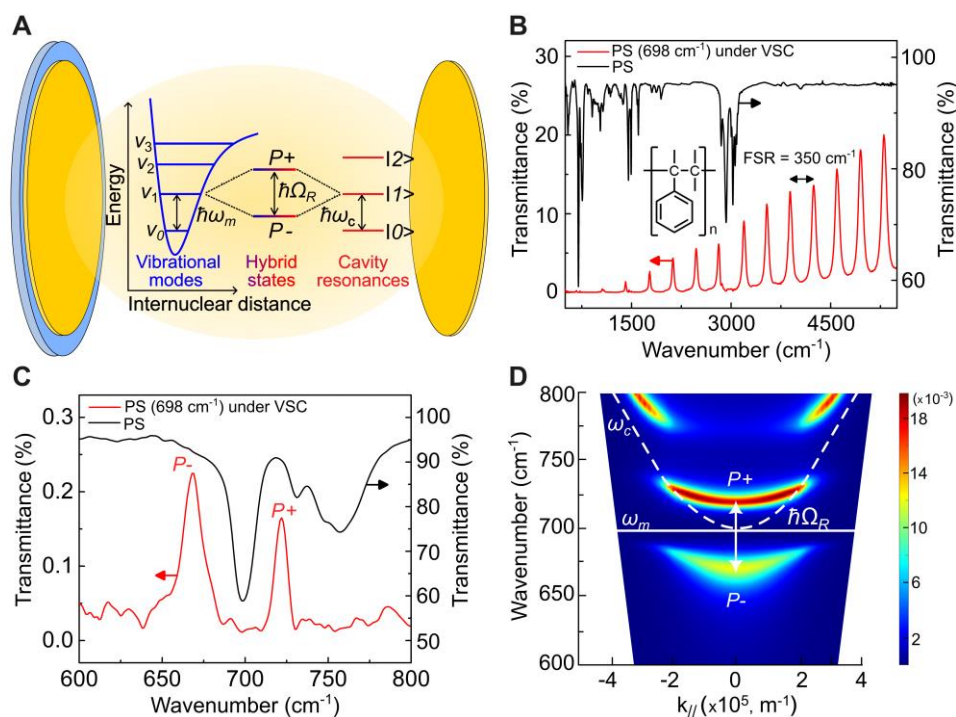


Figure 1. Vibrational strong coupling of polystyrene out-of-plane bending mode (698 cm⁻¹). (A) Schematic illustration of the VSC between molecular transition and cavity mode forming the polaritonic states (P⁺ and P⁻) separated by $\hbar\Omega_R$. (B) Infrared transmission spectrum of strongly coupled PS (red) and a thin film of PS (black). The inset shows the schematic structure of PS. (C) The zoom of the range in B shows the 698 cm⁻¹ vibrational transition of PS (black) and its splitting under VSC (red), resulting in the polaritonic peaks P⁺ and P⁻. (D) The simulated dispersion diagram of the strongly coupled PS shows the avoided crossing. The dashed white curve represents the dispersion of the uncoupled cavity mode, and the solid white line corresponds to the energy of the PS vibrational mode (698 cm⁻¹).

The atactic PS used in our experiments shows strong infrared bands (Fig. 1B, black) that can be directly strongly coupled: out-of-plane bending of the aromatic ring (542 cm⁻¹, 698 cm⁻¹, and 756 cm⁻¹), deformation of CH₂ (1452 cm⁻¹), the ring in-plane stretching (1492 cm⁻¹) and C-H

asymmetrical stretching (2924 cm^{-1}).³¹ To check the influence of VSC on electrical conductance, we first studied the role of the strongest out-of-plane bending transition of PS (698 cm^{-1}), as such modes assist vibronic coupling in aromatic molecules.²⁹ The red curve in Fig. 1B shows the infrared transmission spectrum of the strongly coupled cavity ($\sim 9\text{ }\mu\text{m}$ thick), whose second mode is on-resonance with the 698 cm^{-1} PS vibration. VSC splits PS transition (black curve) into the lower (P-) and higher (P+) energy polariton bands (red curve, Fig. 1C) separated by $\hbar\Omega_R$ (53 cm^{-1}), which is larger than the FWHM of both the cavity mode (20 cm^{-1}) and the PS vibration (16 cm^{-1}). The clear anti-crossing of the polariton peaks in the simulated angle-dependent dispersion of the coupled cavity and the excellent correlation between experimental and calculated $\hbar\Omega_R$ (53 cm^{-1}) confirms the formation of the hybrid light-matter states.

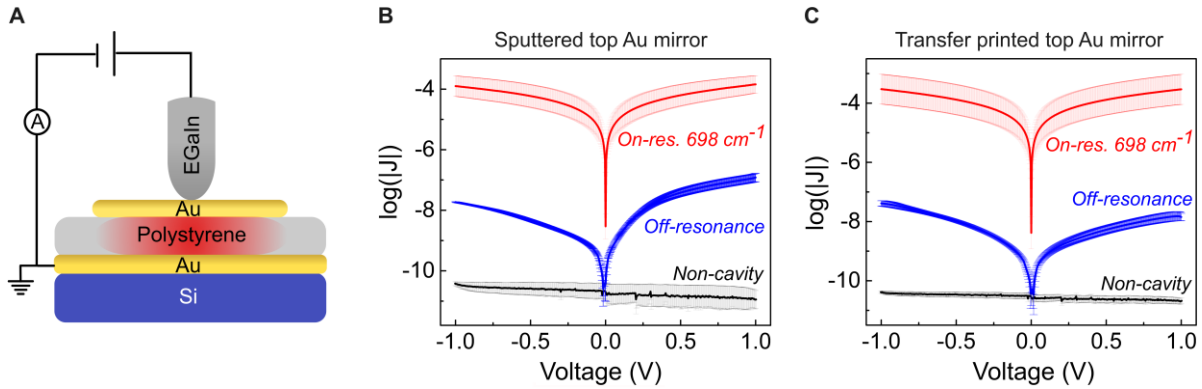


Figure 2. Electrical conductance characteristics of PS under VSC. (A) Schematic representation of the electrical transport measurement setup. (B) The J-V curve correspond strongly coupled PS under cavity VSC (red curve, 698 cm^{-1} vibrational transition of PS), under off-resonance (blue curve), and non-cavity (black curve). The cavities are closed by sputtering the top Au mirror. (C) The J-V curves of PS embedded cavities closed by transfer printing the top Au mirror; strongly coupled PS (red curve), off-resonance (blue curve), and non-cavity (black curve). Here the non-cavity refers to the measurements done at a top mirrorless region of the on-resonance sample. The solid line in all the curves represents the statistically significant master curve extracted from 720 sweeps, and the thin lines show the distribution's standard deviation.

A eutectic mixture of gallium and indium (EGaIn) is used as the probe to measure the electrical conductance properties of strongly coupled PS. The liquid metal electrode allows us to make soft contact³² with the top Au mirror of the cavity without deforming it (Fig. 2A). Connecting a Cu probe to the bottom Au mirror completes the measurement circuit. The PS thickness was larger than $3\text{ }\mu\text{m}$ in nearly all the samples, eliminating the chance of any short circuit.³³ We studied the electrical conductance by measuring the I-V with a bias voltage window of +1 to -1 V in at least six different junctions with a minimum of 60 cycles (60 forward and 60 backward sweeps) at each

junction in the homogenous region of the cavity to get the statistically significant I-V data.³⁴ The plot of mirror area normalized current density ($|J|$) against voltage (J-V curve) given in Fig.2B and 2C is the statistically significant master curve extracted from six different junctions (6 x120 curves). Supplementary Materials provide the details of the EGaIn-assisted electrical measurements and data analysis procedure.

Vibrational strong coupling of the 698 cm^{-1} vibrational mode of PS results in a surprisingly high value of current density, $\sim 1 \times 10^{-4}\text{ Acm}^{-2}$ at $\pm 1\text{ V}$ (Fig.2B, red curve) which is six orders magnitude higher than the non-cavity PS ($5 \times 10^{-11}\text{ Acm}^{-2}$ at $\pm 1\text{ V}$; Fig. 2B, black curve). The non-cavity PS may have an even lower current density³⁵ than our observation, as it is the limit of detection of our current measurement system (Fig. S5). To verify the extraordinary enhancement of electrical conductance is a VSC effect, we investigated the current density through off-resonance PS samples (vibrational transitions of PS detuned from cavity modes). The blue curve in Fig. 2B shows the J-V curve of an off-resonance PS with a cavity path length of $7\text{ }\mu\text{m}$. The current density ($\sim 2 \times 10^{-8}\text{ A cm}^{-2}$ at -1 V) is nearly four orders of magnitude less than the vibrationally strongly coupled PS (698 cm^{-1}) but approximately three orders higher than non-cavity PS. We used deuterated polystyrene (PS- d_8) to assess if the existence of a cavity mode at 698 cm^{-1} alone can lead to extraordinary enhancement in conductance. Deuterium substitution redshifts the corresponding vibrational frequencies. For instance, the 698 cm^{-1} out-of-plane bending transition of PS shifts to 550 cm^{-1} in PS- d_8 (Fig.S8), resulting in a vibrational mode-free window around 698 cm^{-1} . By tuning the cavity resonance to be present at 698 cm^{-1} in a PS- d_8 -filled cavity, we show that the cavity mode in the absence of VSC does not induce extraordinary electrical conductance (Fig. S8).

Further, we prepared a series of cavities where the top mirror deposition is through the transfer printing method using poly(dimethyl siloxane) (PDMS).³⁶ Here the Au (50 nm thick) sputtered on a PDMS slab is transferred onto the PS by stamping technique. Subsequent PDMS slab peeling off leaves the Au mirror on top of PS, forming the cavity. The electrical characterization data of a set of on- and off-resonance PS cavities prepared following the Au transfer printing method (Fig. 2C and Fig.S9-S18) resembles the J-V curves of cavities prepared by sputtering Au mirror on top of PS. Refer to supplementary materials for details of Au transfer printing, optical and electrical characterization of the ten such cavities prepared (Fig.S9-S18). This additional control experiment establishes that the observed extraordinary electrical conductance is independent of sputtering artifacts.

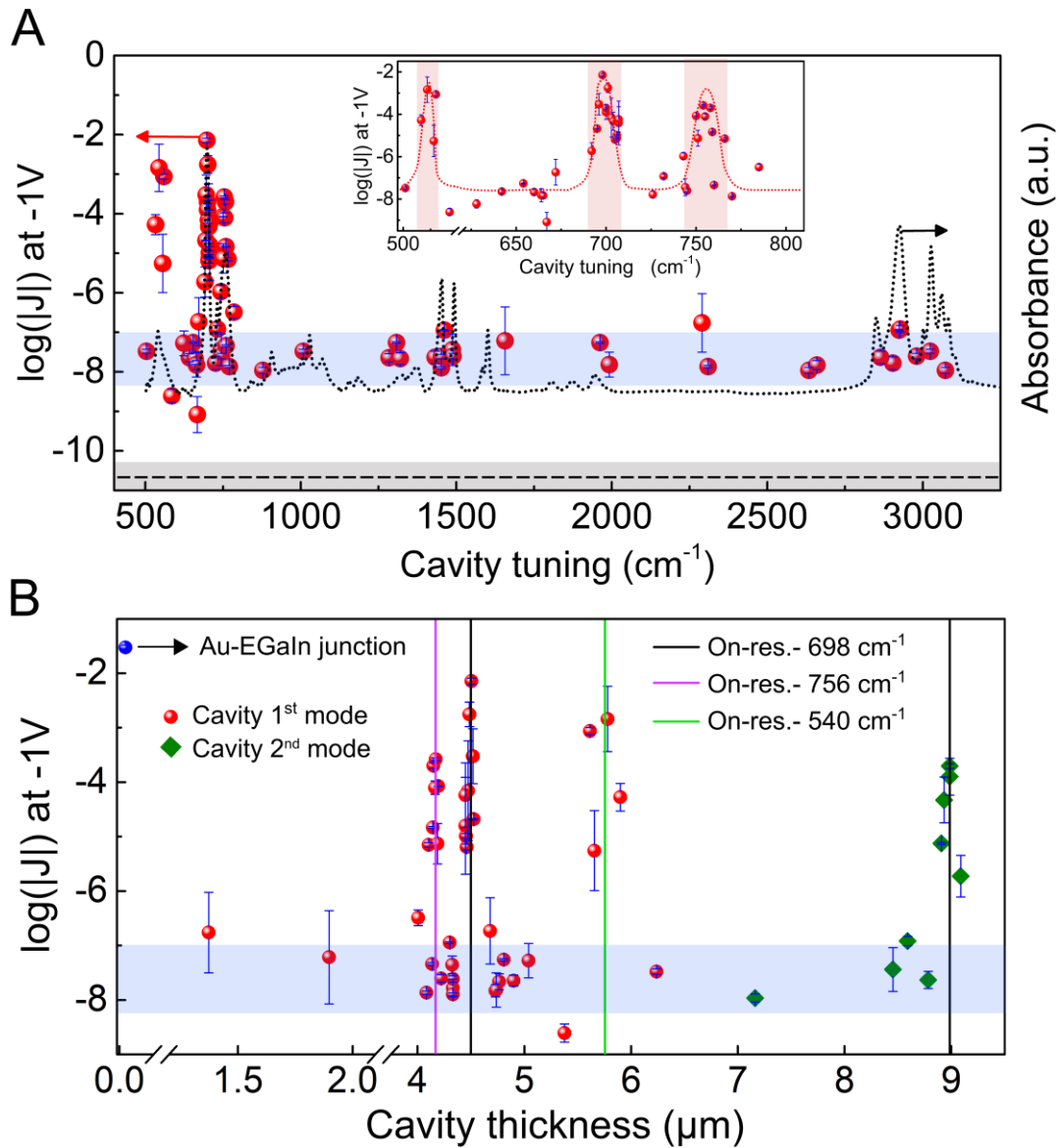


Figure 3. Electrical conductance through PS as a function of cavity tuning and thickness. (A) Cavity action spectrum showing the impact of VSC of different vibrational modes on electrical conductance. The red spheres indicate the cavity mode position. The blue-shaded region highlights the conductance of off-resonance and strongly coupled non- B_2 symmetry modes of PS. The black dashed line shows the measured current density value of non-cavity PS with standard deviation shaded in grey. The black dotted line shows the infrared absorption of PS. The inset shows the region of the B_2 -symmetry modes of PS. The red-shaded area in the inset corresponds to the FWHM of each B_2 symmetry mode studied. The red dotted curve in the inset is a guide to the eye showing the resonance effect of enhanced electrical conductance. (B) The plot of current density as a function of cavity thickness. The black, pink, and green solid vertical lines indicate the resonance condition for cavity VSC of the three different PS vibrational transitions with B_2 symmetry. The red spheres and green diamonds indicate that the PS is strongly coupled to the first or second mode of the cavity, respectively. The blue sphere represents the current density of the Au-EGaIn shorted junction.

To check the vibrational mode selectivity and to better understand the origin of conductance under off-resonance and its variation from the on-resonance and non-cavity, we probed the role of other PS vibrational transitions by tuning the position of cavity modes. The cavity action spectrum in Fig. 3A acquired from more than 50 different cavities shows the impact of the VSC on different vibrational modes of PS in modifying the electrical conductance. VSC of the three out-of-plane bending modes (698 cm^{-1} , 756 cm^{-1} , and 540 cm^{-1}) induces extraordinary enhancement of electrical conductance ($|J| \sim 10^{-4}\text{ A cm}^{-2}$). However, the VSC of 1452 cm^{-1} , 1492 cm^{-1} , and 2924 cm^{-1} PS vibrations yields current density in the range of 10^{-8} to 10^{-7} A cm^{-2} (blue shaded region in Fig. 3A) similar to off-resonance.

Treating PS as monosubstituted benzene, in localized symmetry terms, the C_{2v} point group is assigned.³¹ Then the out-of-plane bending modes belong to B_2 symmetry and have the transition moments perpendicular to the plane of the benzene ring, while that of 1452 cm^{-1} and 1493 cm^{-1} bands are in the plane of the ring with B_1 and A_1 symmetry, respectively.³¹ The 2924 cm^{-1} C-H asymmetric stretching is also an in-plane vibration. Often, out-of-plane vibrations result in vibronic mixing, whereas in-plane vibrations undergo adiabatic coupling.²⁹ The apparent correlation between extraordinary enhancement in electrical conductance and VSC of the out-of-plane bending modes (Fig. 3A inset) indicates that vibronic coupling in PS could be a prerequisite. In Fig. 3B, we plot the dependence of measured current density vs. cavity thickness. Remarkably, the extraordinary enhancement in electrical conductance through PS is only dependent on the VSC of the B_2 symmetry vibrations and is independent of the order of the cavity modes and therefore of the cavity thickness. The spectral and electrical analysis data of all the samples prepared and analyzed are given in Supplementary Materials (Fig.S24 -S62).

As the non- B_2 symmetry modes of PS do not participate in vibronic mixing, the VSC of those modes and off-resonance PS should have a similar conductance as seen in our experiments. However, the improved electrical conductance in the latter compared to non-cavity PS (the blue- and the grey-shaded area in Fig. 3A, respectively) indicates the presence of surface plasmon coupling to the mirror dipoles of PS. Such interaction is typical when a molecule is placed on top of smooth flat metal surfaces and can reach the strong coupling regime if the molecular absorption is large enough,³⁷ as observed earlier for PS.¹² Albeit surface plasmon can strongly couple to different PS vibrational modes, its role in improved electrical conductance would be limited to the interaction with B_2 symmetry vibrational transition. In an off-resonance cavity, both the flat Au

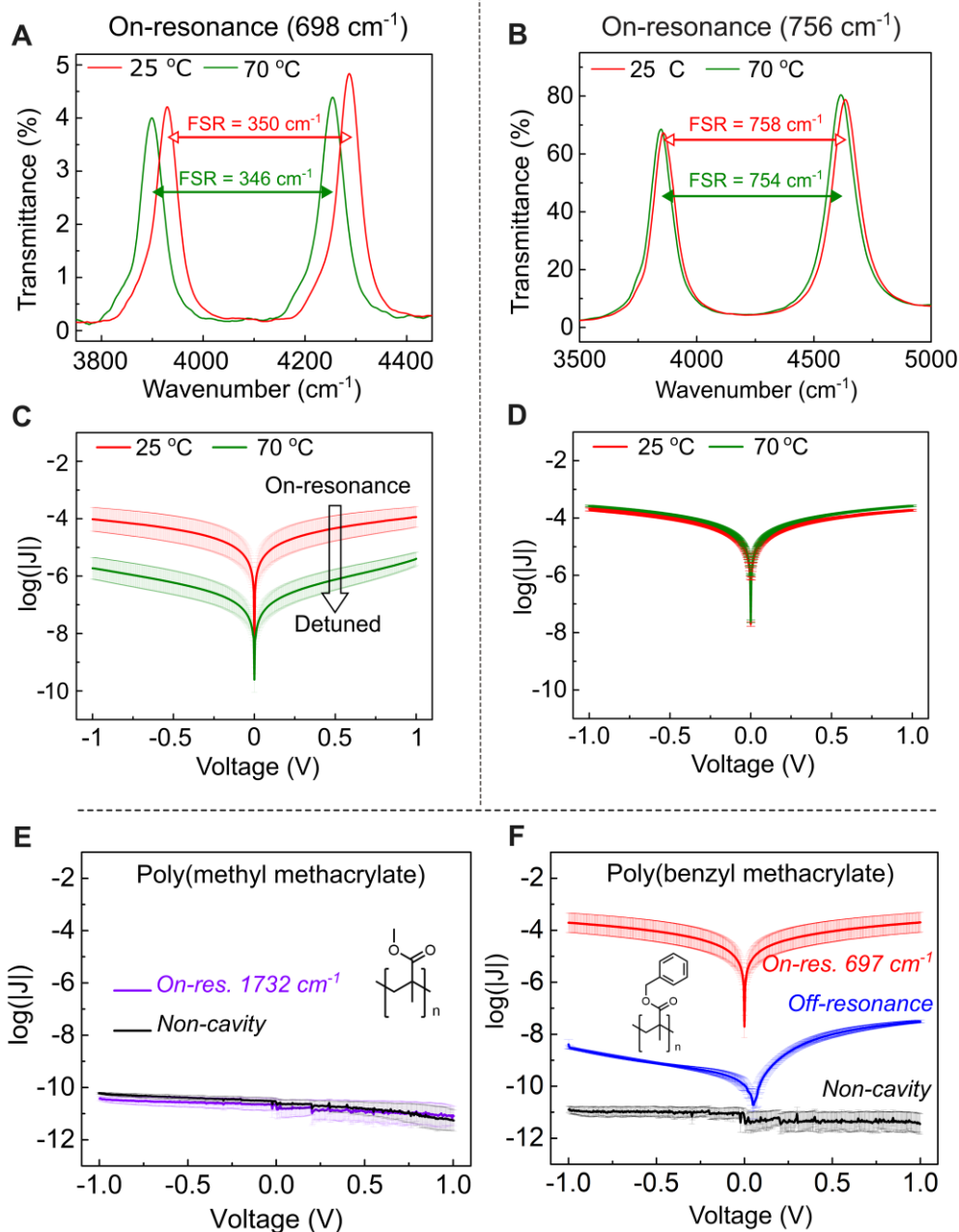


Figure 4. Evidence for the role of cavity VSC on the extraordinary enhancement of electrical conductance through PS and PBMA. (A) A high energy region of the infrared transmission spectra of the cavity where its second mode on-resonance with the 698 cm^{-1} vibrational transition of PS at $25\text{ }^{\circ}\text{C}$ (red curve) and $70\text{ }^{\circ}\text{C}$ (green curve) showing the reduction in FSR upon heating. (B) Represent the FSR change upon heating a cavity where its first mode is on-resonance with the 758 cm^{-1} vibrational transition of PS: red curve (at $25\text{ }^{\circ}\text{C}$) and green curve (at $70\text{ }^{\circ}\text{C}$). (C, D) The J-V curves at $25\text{ }^{\circ}\text{C}$ (red curve) and $70\text{ }^{\circ}\text{C}$ (green curve) of the strongly coupled PS. The downward arrow shows the trend of conductance upon detuning due to heating. (E) The J-V curve corresponds to PMMA under cavity VSC (violet curve, 1732 cm^{-1} C=O stretching transition) and non-cavity (black curve). (F) The J-V curve corresponds to strongly coupled PBMA (aromatic ring out-of-plane bending transition- 697 cm^{-1} ; red curve), off-resonance (blue curve), and non-cavity (black curve).

mirrors can support surface plasmons to which the PS can strongly couple. Nevertheless, the evanescent nature of the plasmons and other losses, in particular from Au, in the IR³⁸ reduces the fraction of strongly coupled molecules, as primarily transition dipoles close to the PS-Au interfaces are coupled, leading to a reduced electrical conductance compared to an on-resonance cavity. The plasmonic field becomes minimal at the PS surface in non-cavity (~9 μm thick layer of PS), where the polymer experiences no net enhancement of electrical conductance.

Further, we detuned an on-resonance cavity *in-situ* by heating (70°C) to confirm the correlation between cavity-VSC and extraordinary electrical conductance. Heating expands the polymer, causing a slight increase in the cavity path length, reducing its free spectral range (FSR) and red shifting the modes (Fig. 4A, B). For instance, the FSR (350 cm^{-1} at 25 °C) of the cavity on-resonance with the 698 cm^{-1} PS vibration (Fig. 4A, red curve) is lowered to 346 cm^{-1} at 70 °C (Fig. 4A, blue curve) detuning the second mode of cavity away from resonance to 692 cm^{-1} . As a result, the conductance drops two orders of magnitude (Fig. 4C). Cooling down the cavity to 25 °C, fetches the on-resonance condition and the enhanced conductance, as shown in Fig. S19B. In Fig.4C and D, we show the spectral and electrical characterization data of a cavity whose first mode (FSR=758 cm^{-1}) is on-resonance with another B_2 vibration (756 cm^{-1}) of PS. Although heating changes the FSR to 754 cm^{-1} , the cavity resonance is still inside the effective width of PS vibration (FWHM= 25 cm^{-1}); hence no change in conductance is observed (Fig. 4D, Fig.S19C). We repeated the *in-situ* heating-cooling cycle three times, presenting unequivocal evidence for the role of cavity VSC in the extraordinary enhancement of conductance. On the other hand, in off-resonance cavities, PS conductance increases when heated to 70°C (Fig. S19D). The strong coupling of surface plasmon modes with a matter transition is an interfacial interaction and should not be affected by the slight PS thickness variation due to heating.

To check if there is any molecular weight dependence, we conducted experiments using higher (Mw = 292000) and lower (Mw = 35000) molecular weight PS purchased from a different origin. Independent of the molecular weight and source, the strongly coupled PS (B_2 modes) showed extraordinary enhancement in electrical conductance (Fig.S20 and S21).

To benchmark the need for vibronic mixing, we conducted experiments by strongly coupling the vibrational modes of poly(methyl methacrylate) (PMMA), a polymer with only aliphatic chains and no aromatic units that support vibronic coupling.²⁹ PMMA remained as an insulator even under

the VSC as shown in Fig.4E. Even though PMMA vibrations can couple to the surface plasmon modes, the absence of any improvement in conductance confirms the requirement of a vibrational transition facilitating the vibronic coupling. Additionally, experiments with PMMA suggest that the Au mirrors do not contribute to the electrical transport as an impurity.

To validate the generality of our observations, we studied the electrical conductance properties of PBMA, a polymer having pendant benzene rings akin to PS. Interestingly, PBMA also shows the extraordinary enhancement in conductance under the VSC of its aromatic ring out-of-plane bending vibration (697 cm^{-1} , Fig.4F). Remarkably, these observations point to a general phenomenon where VSC can be a tool to tune the conductance properties of non-conducting polymers. Refer to Supplementary Materials for further details.

Through the current experiments, we show, for the first time, that VSC of the vibrational mode greatly enhances the electrical conductance through undoped PS and PBMA, polymers that are otherwise non-conductors. This extraordinary enhancement of electrical conductance through PS and PBMA under VSC could be related to a process that modifies the hopping. It has been shown that the long-range correlations under electronic strong coupling can expand the transport mean free path leading to enhanced diffusion and overcome the molecular disorder at large coupling strengths.^{18,39,40} In organic semiconductors, vibronic coherences circumvent the disorder and dissipation to enhance charge transport by adopting a coherent wave-like transport.^{21,27} Since the out-of-plane bending vibrational modes are known to facilitate non-adiabatic vibronic mixing,²⁹ it is reasonable to assume that the delocalized vibro-polaritonic states lead to vibronic quantum coherence in PS and PBMA under VSC.^{14,41} Therefore, VSC could induce quantum coherent wave packet-like transport in PS and PBMA, resulting in extraordinary electrical conductance. Nevertheless, the present observation and the nature of states under VSC demand a thorough theoretical investigation. Remarkably, enhancement in the electrical conductance through PS and PBMA depends on the ability of the vibrations to promote vibronic mixing, providing a mode-selective character. Interestingly, the nature of the J vs. V plot (Fig. 2B, blue curve) is asymmetric when strongly coupled to surface plasmons. Albeit the origin is unclear at this stage, it has been a feature in many experiments where the electrical conductance is probed under the influence of a plasmonic field.^{14,16,42,43}

Remarkably, we show that one can transform the non-conducting amorphous polymers (PS and PBMA) into a conductor by simply placing them between two mirrors at the right distance. VSC

provides a handle to tune the electrical conductance through molecular materials, which is thickness independent if the strong coupling is maintained. The device preparation is straightforward, providing another platform for lossless quantum transport and long-range energy transport in molecular devices. In addition to modified chemical dynamics,^{7,44} enhanced ionic conductivity,¹¹ and magnetism,¹² it is clear that VSC also offers completely new possibilities for organic electronics and semiconductor technology.

References

- (1) Haroche, S.; Kleppner, D. Cavity Quantum Electrodynamics. *Phys. Today* **1989**, *42* (1), 24. <https://doi.org/10.1063/1.881201>.
- (2) Riek, C.; Seletskiy, D. V.; Moskalenko, A. S.; Schmidt, J. F.; Krauspe, P.; Eckart, S.; Eggert, S.; Burkard, G.; Leitenstorfer, A. Direct Sampling of Electric-Field Vacuum Fluctuations. *Science* **2015**, *350* (6259), 420–423. <https://doi.org/10.1126/science.aac9788>.
- (3) Garcia-Vidal, F. J.; Ciuti, C.; Ebbesen, T. W. Manipulating Matter by Strong Coupling to Vacuum Fields. *Science* **2021**, *373* (6551). <https://doi.org/10.1126/science.abd0336>.
- (4) Thomas, A.; George, J.; Shalabney, A.; Dryzhakov, M.; Varma, S. J.; Moran, J.; Chervy, T.; Zhong, X.; Devaux, E.; Genet, C.; Hutchison, J. A.; Ebbesen, T. W. Ground-State Chemical Reactivity under Vibrational Coupling to the Vacuum Electromagnetic Field. *Angew. Chem. Int. Ed.* **2016**, *55* (38), 11462–11466. <https://doi.org/10.1002/anie.201605504>.
- (5) Appugliese, F.; Enkner, J.; Paravicini-Bagliani, G. L.; Beck, M.; Reichl, C.; Wegscheider, W.; Scalari, G.; Ciuti, C.; Faist, J. Breakdown of Topological Protection by Cavity Vacuum Fields in the Integer Quantum Hall Effect. *Science* **2022**, *375* (6584), 1030–1034. <https://doi.org/10.1126/science.abl5818>.
- (6) Genet, C.; Faist, J.; Ebbesen, T. W. Inducing New Material Properties with Hybrid Light–Matter States. *Phys. Today* **2021**, *74* (5), 42–48. <https://doi.org/10.1063/PT.3.4749>.
- (7) Thomas, A.; Lethuillier-Karl, L.; Nagarajan, K.; Vergauwe, R. M. A.; George, J.; Chervy, T.; Shalabney, A.; Devaux, E.; Genet, C.; Moran, J.; Ebbesen, T. W. Tilting a Ground-State Reactivity Landscape by Vibrational Strong Coupling. *Science* **2019**, *363* (6427), 615–619. <https://doi.org/10.1126/science.aau7742>.
- (8) Dunkelberger, A. D.; Simpkins, B. S.; Vurgaftman, I.; Owrutsky, J. C. Vibration-Cavity Polariton Chemistry and Dynamics. *Annu. Rev. Phys. Chem.* **2022**, *73* (1), 429–451. <https://doi.org/10.1146/annurev-physchem-082620-014627>.
- (9) Pang, Y.; Thomas, A.; Nagarajan, K.; Vergauwe, R. M. A.; Joseph, K.; Patrahau, B.; Wang, K.; Genet, C.; Ebbesen, T. W. On the Role of Symmetry in Vibrational Strong Coupling: The Case of Charge-Transfer Complexation. *Angew. Chem. Int. Ed.* **2020**, *59* (26), 10436–10440. <https://doi.org/10.1002/anie.202002527>.
- (10) Hirai, K.; Ishikawa, H.; Chervy, T.; Hutchison, J. A.; Uji-i, H. Selective Crystallization via Vibrational Strong Coupling. *Chem. Sci.* **2021**, *12* (36), 11986–11994. <https://doi.org/10.1039/D1SC03706D>.
- (11) Fukushima, T.; Yoshimitsu, S.; Murakoshi, K. Inherent Promotion of Ionic Conductivity via Collective Vibrational Strong Coupling of Water with the Vacuum Electromagnetic

- Field. *J. Am. Chem. Soc.* **2022**, *144* (27), 12177–12183.
<https://doi.org/10.1021/jacs.2c02991>.
- (12) Thomas, A.; Devaux, E.; Nagarajan, K.; Rogez, G.; Seidel, M.; Richard, F.; Genet, C.; Drillon, M.; Ebbesen, T. W. Large Enhancement of Ferromagnetism under a Collective Strong Coupling of YBCO Nanoparticles. *Nano Lett.* **2021**, *21* (10), 4365–4370.
<https://doi.org/10.1021/acs.nanolett.1c00973>.
- (13) Paravicini-Bagliani, G. L.; Appugliese, F.; Richter, E.; Valmorra, F.; Keller, J.; Beck, M.; Bartolo, N.; Rössler, C.; Ihn, T.; Ensslin, K.; Ciuti, C.; Scalari, G.; Faist, J. Magneto-Transport Controlled by Landau Polariton States. *Nat. Phys.* **2019**, *15* (2), 186–190.
<https://doi.org/10.1038/s41567-018-0346-y>.
- (14) Orgiu, E.; George, J.; Hutchison, J. A.; Devaux, E.; Dayen, J. F.; Doudin, B.; Stellacci, F.; Genet, C.; Schachenmayer, J.; Genes, C.; Pupillo, G.; Samorì, P.; Ebbesen, T. W. Conductivity in Organic Semiconductors Hybridized with the Vacuum Field. *Nat. Mater.* **2015**, *14* (11), 1123–1129. <https://doi.org/10.1038/nmat4392>.
- (15) Krainova, N.; Grede, A. J.; Tsokkou, D.; Banerji, N.; Giebink, N. C. Polaron Photoconductivity in the Weak and Strong Light-Matter Coupling Regime. *Phys. Rev. Lett.* **2020**, *124* (17), 177401. <https://doi.org/10.1103/PhysRevLett.124.177401>.
- (16) Nagarajan, K.; George, J.; Thomas, A.; Devaux, E.; Chervy, T.; Azzini, S.; Joseph, K.; Jouaiti, A.; Hosseini, M. W.; Kumar, A.; Genet, C.; Bartolo, N.; Ciuti, C.; Ebbesen, T. W. Conductivity and Photoconductivity of a P-Type Organic Semiconductor under Ultrastrong Coupling. *ACS Nano* **2020**, *14* (8), 10219–10225. <https://doi.org/10.1021/acsnano.0c03496>.
- (17) Bhatt, P.; Kaur, K.; George, J. Enhanced Charge Transport in Two-Dimensional Materials through Light–Matter Strong Coupling. *ACS Nano* **2021**, *15* (8), 13616–13622.
<https://doi.org/10.1021/acsnano.1c04544>.
- (18) Balasubrahmaniam, M.; Simkhovich, A.; Golombek, A.; Sandik, G.; Ankonina, G.; Schwartz, T. From Enhanced Diffusion to Ultrafast Ballistic Motion of Hybrid Light–Matter Excitations. *Nat. Mater.* **2023**, *22* (3), 338–344. <https://doi.org/10.1038/s41563-022-01463-3>.
- (19) Schäfer, C.; Ruggenthaler, M.; Appel, H.; Rubio, A. Modification of Excitation and Charge Transfer in Cavity Quantum-Electrodynamical Chemistry. *Proc. Natl. Acad. Sci.* **2019**, *116* (11), 4883–4892. <https://doi.org/10.1073/pnas.1814178116>.
- (20) Hagenmüller, D.; Schachenmayer, J.; Schütz, S.; Genes, C.; Pupillo, G. Cavity-Enhanced Transport of Charge. *Phys. Rev. Lett.* **2017**, *119* (22), 223601.
<https://doi.org/10.1103/PhysRevLett.119.223601>.
- (21) Sio, A. D.; Lienau, C. Vibronic Coupling in Organic Semiconductors for Photovoltaics. *Phys. Chem. Chem. Phys.* **2017**, *19* (29), 18813–18830.
<https://doi.org/10.1039/C7CP03007J>.
- (22) Falke, S. M.; Rozzi, C. A.; Brida, D.; Maiuri, M.; Amato, M.; Sommer, E.; De Sio, A.; Rubio, A.; Cerullo, G.; Molinari, E.; Lienau, C. Coherent Ultrafast Charge Transfer in an Organic Photovoltaic Blend. *Science* **2014**, *344* (6187), 1001–1005.
<https://doi.org/10.1126/science.1249771>.
- (23) Rini, M.; Tobey, R.; Dean, N.; Itatani, J.; Tomioka, Y.; Tokura, Y.; Schoenlein, R. W.; Cavalleri, A. Control of the Electronic Phase of a Manganite by Mode-Selective Vibrational Excitation. *Nature* **2007**, *449* (7158), 72–74. <https://doi.org/10.1038/nature06119>.
- (24) Bakulin, A. A.; Rao, A.; Pavelyev, V. G.; van Loosdrecht, P. H. M.; Pshenichnikov, M. S.; Niedzialek, D.; Cornil, J.; Beljonne, D.; Friend, R. H. The Role of Driving Energy and Delocalized States for Charge Separation in Organic Semiconductors. *Science* **2012**, *335* (6074), 1340–1344. <https://doi.org/10.1126/science.1217745>.

- (25) Bakulin, A. A.; Lovrincic, R.; Yu, X.; Selig, O.; Bakker, H. J.; Rezus, Y. L. A.; Nayak, P. K.; Fonari, A.; Coropceanu, V.; Brédas, J.-L.; Cahen, D. Mode-Selective Vibrational Modulation of Charge Transport in Organic Electronic Devices. *Nat. Commun.* **2015**, *6*, 7880. <https://doi.org/10.1038/ncomms8880>.
- (26) Delor, M.; Sazanovich, I. V.; Towrie, M.; Weinstein, J. A. Probing and Exploiting the Interplay between Nuclear and Electronic Motion in Charge Transfer Processes. *Acc. Chem. Res.* **2015**, *48* (4), 1131–1139. <https://doi.org/10.1021/ar500420c>.
- (27) Scholes, G. D.; Fleming, G. R.; Chen, L. X.; Aspuru-Guzik, A.; Buchleitner, A.; Coker, D. F.; Engel, G. S.; van Grondelle, R.; Ishizaki, A.; Jonas, D. M.; Lundeen, J. S.; McCusker, J. K.; Mukamel, S.; Ogilvie, J. P.; Olaya-Castro, A.; Ratner, M. A.; Spano, F. C.; Whaley, K. B.; Zhu, X. Using Coherence to Enhance Function in Chemical and Biophysical Systems. *Nature* **2017**, *543* (7647), 647–656. <https://doi.org/10.1038/nature21425>.
- (28) Chattopadhyay, S.; Datta, A.; Giglia, A.; Mahne, N.; Das, A.; Nannarone, S. Intramolecular and Intermolecular Rearrangements in Nanoconfined Polystyrene. *Macromolecules* **2007**, *40* (25), 9190–9196. <https://doi.org/10.1021/ma071392y>.
- (29) Turro, N. J.; Ramamurthy, V.; Scaiano, J. C. *Modern Molecular Photochemistry of Organic Molecules*. University Science Books. <https://uscibooks.aip.org/books/modern-molecular-photochemistry-of-organic-molecules/> (accessed 2022-07-22).
- (30) Chattopadhyay, S.; Datta, A. Effect of Polymer Confinement: Tuning Self-Assembled Growth of Monodisperse Au Nanoparticles on Polystyrene Films. *Macromolecules* **2007**, *40* (9), 3313–3319. <https://doi.org/10.1021/ma0624088>.
- (31) Liang, C. Y.; Krimm, S. Infrared Spectra of High Polymers. VI. Polystyrene. *J. Polym. Sci.* **1958**, *27* (115), 241–254. <https://doi.org/10.1002/pol.1958.1202711520>.
- (32) Chiechi, R. C.; Weiss, E. A.; Dickey, M. D.; Whitesides, G. M. Eutectic Gallium–Indium (EGaIn): A Moldable Liquid Metal for Electrical Characterization of Self-Assembled Monolayers. *Angew. Chem. Int. Ed.* **2008**, *47* (1), 142–144. <https://doi.org/10.1002/anie.200703642>.
- (33) McCreery, R. L.; Bergren, A. J. Progress with Molecular Electronic Junctions: Meeting Experimental Challenges in Design and Fabrication. *Adv. Mater.* **2009**, *21* (43), 4303–4322. <https://doi.org/10.1002/adma.200802850>.
- (34) Atesci, H.; Kaliginedi, V.; Celis Gil, J. A.; Ozawa, H.; Thijssen, J. M.; Broekmann, P.; Haga, M.; van der Molen, S. J. Humidity-Controlled Rectification Switching in Ruthenium-Complex Molecular Junctions. *Nat. Nanotechnol.* **2018**, *13* (2), 117–121. <https://doi.org/10.1038/s41565-017-0016-8>.
- (35) Kamisako, K.; Akiyama, S.; Shinohara, K. Electrical Conduction of Polystyrene Films. *Jpn. J. Appl. Phys.* **1974**, *13* (11), 1780. <https://doi.org/10.1143/JJAP.13.1780>.
- (36) Meitl, M. A.; Zhu, Z.-T.; Kumar, V.; Lee, K. J.; Feng, X.; Huang, Y. Y.; Adesida, I.; Nuzzo, R. G.; Rogers, J. A. Transfer Printing by Kinetic Control of Adhesion to an Elastomeric Stamp. *Nat. Mater.* **2006**, *5* (1), 33–38. <https://doi.org/10.1038/nmat1532>.
- (37) Rider, M. S.; Arul, R.; Baumberg, J. J.; Barnes, W. L. Theory of Strong Coupling between Molecules and Surface Plasmons on a Grating. *Nanophotonics* **2022**, *11* (16), 3695–3708. <https://doi.org/10.1515/nanoph-2022-0301>.
- (38) Stanley, R. Plasmonics in the Mid-Infrared. *Nat. Photonics* **2012**, *6* (7), 409–411. <https://doi.org/10.1038/nphoton.2012.161>.
- (39) Aberra Guebrou, S.; Symonds, C.; Homeyer, E.; Plenet, J. C.; Gartstein, Yu. N.; Agranovich, V. M.; Bellessa, J. Coherent Emission from a Disordered Organic Semiconductor Induced by Strong Coupling with Surface Plasmons. *Phys. Rev. Lett.* **2012**, *108* (6), 066401. <https://doi.org/10.1103/PhysRevLett.108.066401>.

- (40) Shi, L.; Hakala, T. K.; Rekola, H. T.; Martikainen, J.-P.; Moerland, R. J.; Törmä, P. Spatial Coherence Properties of Organic Molecules Coupled to Plasmonic Surface Lattice Resonances in the Weak and Strong Coupling Regimes. *Phys. Rev. Lett.* **2014**, *112* (15), 153002. <https://doi.org/10.1103/PhysRevLett.112.153002>.
- (41) Dubail, J.; Botzung, T.; Schachenmayer, J.; Pupillo, G.; Hagenmüller, D. Large Random Arrowhead Matrices: Multifractality, Semilocalization, and Protected Transport in Disordered Quantum Spins Coupled to a Cavity. *Phys. Rev. A* **2022**, *105* (2), 023714. <https://doi.org/10.1103/PhysRevA.105.023714>.
- (42) Ward, D. R.; Hüser, F.; Pauly, F.; Cuevas, J. C.; Natelson, D. Optical Rectification and Field Enhancement in a Plasmonic Nanogap. *Nat. Nanotechnol.* **2010**, *5* (10), 732–736. <https://doi.org/10.1038/nnano.2010.176>.
- (43) Arielly, R.; Ofarim, A.; Noy, G.; Selzer, Y. Accurate Determination of Plasmonic Fields in Molecular Junctions by Current Rectification at Optical Frequencies. *Nano Lett.* **2011**, *11* (7), 2968–2972. <https://doi.org/10.1021/nl201517k>.
- (44) Chen, T.-T.; Du, M.; Yang, Z.; Yuen-Zhou, J.; Xiong, W. Cavity-Enabled Enhancement of Ultrafast Intramolecular Vibrational Redistribution over Pseudorotation. *Science* **2022**, *378* (6621), 790–794. <https://doi.org/10.1126/science.add0276>.

Acknowledgments: We thank the Department of Inorganic and Physical Chemistry, Center for Nanoscience and Engineering, Dr. P. Rajamalli, and Prof. S. Ramakrishnan for providing access to instrumentation facilities. We thank Prof. S. Vasudevan for gifting us deuterated polystyrene. SB, UR, and KSM thank DST-INSPIRE and Prime Minister’s Research Fellowship (PMRF) for the Ph.D. fellowship. SK thanks UGC for the research fellowship. RV thanks the European Research Executive Agency for funding under the European Union Horizon TMA MSCA Postdoctoral Fellowships – European Fellowships action. AT and VK thanks IISc for a start-up grant and DST-SERB for research funding. AT thanks Infosys Young Investigator Award, and VK thanks DST-INSPIRE Faculty Fellowship. We thank Prof. S. Sampath, Prof. E. Arunan, Prof. P. K. Das, Prof. S.G Ramesh, Dr. T. Chervy, and Dr. E. Devaux for their helpful discussion.

Funding: Horizon TMA MSCA Postdoctoral Fellowship – European Fellowship action (Grant Agreement No 101068621) for RV. IISc start-up grant for VK (SG/MHRD-19-0034 and SR/MHRD-19-0028) and AT (IE/CARE-21-0321 and SR/MHRD-20-0039), SERB-CRG grant for VK (CRG/2020/002302) and AT (CRG/2021/002396), Infosys Young Investigator Award for AT (FG/OTHR-21-1050), INSPIRE Faculty fellowship for VK (DST/INSPIRE/04/2018/002983)

Author contributions: All the authors contributed to the results presented in the paper. AT and VK conceived the idea and supervised the project. SB took the lead in preparing and characterizing all the strongly coupled samples. SK took the lead in the electrical measurements. UR and VK build the EGaIn setup. KSM, SB, and RMAV did the Transfer-Matrix simulations. All the authors analyzed the data, discussed together, and wrote the manuscript.